A theoretical investigation of the laser damage threshold of metal multi-dielectric mirrors for high power ultrashort applications

Bin Wang[1,2] **and Laurent Gallais**[1*]

[1] *Institut Fresnel, CNRS, Aix-Marseille Université, Ecole Centrale Marseille, Campus de St Jérôme, 13013 Marseille, France*
[2] *Department of Applied Physics, Nanjing University of Science & Technology, Nanjing 210094, China*
**laurent.gallais@fresnel.fr*

Abstract: An approach for the theoretical evaluation of the damage threshold in optical interference coatings that combine metal and dielectric films is presented. The model that is used combines a matrix formalism to describe the film system with the two temperatures model that describes the energy transfer and the temperatures of electrons and lattice in a solid submitted to a laser irradiation at the femtosecond time scale. With this approach the thermal consequences due to the ultrafast absorption of the metal film can be evaluated in the multilayer stack for single or multiple pulses. Some applications are presented for the case of broad-band mirrors for ultrashort pulses with low dispersion. Particularly we study the impact of the metal film (metal element, thickness) and the design on the Laser Induced Damage Threshold in the sub picosecond regime.

OCIS codes: (310.0310) Thin films; (320.0320) Ultrafast optics; (140.3330) Laser damage.

References and links

1. B. C. Stuart, M.D. Feit, S. Herman, A. M. Rubenchik, B. W. Shore, and M. D. Perry, "Optical ablation by high-power short-pulse lasers," J. Opt. Soc. Am. B **13,** 459–468 (1996).
2. N. Bonod and J. Néauport, "Optical performance and laser induced damage threshold improvement of diffraction gratings used as compressors in ultra high intensity lasers," Opt. Commun. **260**, 649–655 (2006).
3. F. Canova, O. Uteza, J.-P. Chambaret, M. Flury, S. Tonchev, R. Fechner, and O. Parriaux, "High-efficiency, broad band, high-damage threshold high-index gratings for femtosecond pulse compression," Opt. Express **15**, 15324–15334 (2007).
4. S. Palmier, J. Néauport, N. Baclet, E. Lavastre, and G. Dupuy, "High reflection mirrors for pulse compression gratings," Opt. Express **17**, 20430–20439 (2009).
5. J.H. Bechtel, "Heating of solid targets with laser pulses," J. Appl. Phys. **46**, 1585–1593 (1975).
6. M. Mansipur, G.A. Neville Connell, and J.W. Goodman, "Laser-induced local heating of multilayers," Appl. Opt. **21**, 1106–1114 (1982).
7. L. Gallais and M. Commandré, "Photothermal deflection in multilayer coatings: modeling and experiment," Appl. Opt. **44**, 5230–5238 (2005).
8. S. I. Anisimov, B. L. Kapeliovich, and T. L. Perel'man, "Electron emission from metal surfaces exposed to ultra-short laser pulses," Sov. Phys. JETP **39**, 375–377 (1974).
9. R. Petit, *Ondes Electomagnetiques* (Dunod, 1989).
10. P.B. Corkum, F. Brunel, N.K. Sherman, and T. Srinivasan-Rao, "Thermal responses of metals to ultrashort-pulse laser excitation," Phys. Rev. Lett. **61**, 2686–2689 (1988).

11. Z. Lin, L. V. Zhigilei, and V. Celli, "Electron-phonon coupling and electron heat capacity of metals under conditions of strong electron-phonon nonequilibrium," Phys. Rev. B **77**, 75133–75133 (2008).
12. J. Hohlfeld, S. S. Wellershoff, J. Gdde, U. Conrad, V. Jahnke, and E. Matthias, "Electron and lattice dynamics following optical excitation of metals," Chem. Phys. **251**, 237–258 (2000).
13. Y. Ren, J.K. Chen, and Y. Zhang, "Optical properties and thermal responses of copper films induced by ultrashort-pulsed lasers," J. Appl. Phys. **110**, 113102 (2011).
14. Matlab PDE solver http://www.mathworks.com.
15. M.J. Webber, *Handbook of Optical Materials* (CRC Press, 2003).
16. H.A. Macleod, *Thin-film Optical Filters* (CRC Press, 2001).
17. S. S. Wellershoff, J. Hohlfeld, J. Gdde, and E. Matthias, "The role of electron phonon coupling in femtosecond laser damage of metals," Appl. Phys. A **69**, S99–S107 (1999).
18. J. Kruger, D. Dufft, R. Koter, and A. Hertwig, "Femtosecond laser-induced damage of gold films," Appl. Surf. Sci. **253**, 7815–7819 (2007).
19. Y. Dai, M. He, H. Bian, B. Lu, X. Yan, and G. Ma, "Femtosecond laser nanostructuring of silver film," Appl. Phys. A **106**, 567–574 (2012).
20. M. Kimmel, P. Rambo, R. Broyles, M. Geissel, J. Schwarz, J. Bellum, and B. Atherton, "Optical damage testing at the Z-Backlighter facility at Sandia National Laboratories," Proc. SPIE **7504**, 75041G (2009).
21. L. Gallais, E. Bergeret, B. Wang, M. Guerin, and E. Benevent, "Ultrafast laser ablation of metal films on flexible substrates," submitted.
22. X. Y. Wang, D. M. Riffe, Y.-S. Lee, and M. C. Downer, "Time-resolved electron-temperature measurement in a highly excited gold target using femtosecond thermionic emission," Phys. Rev. B **50**, 8016–8019 (1994).
23. M. Mero, J. Liu, W. Rudolph, D. Ristau, and K. Starke, "Scaling laws of femtosecond laser pulse induced breakdown in oxide films," Phys. Rev. B **71**, 115109 (2005).
24. B. Mangote, L. Gallais, M. Commandré, M. Mende, L. Jensen, H. Ehlers, M. Jupé, D. Ristau, A. Melninkaitis, J. Mirauskas, V. Sirutkaitis, S. Kicas, T. Tolenis, and R. Drazdys, "Femtosecond laser damage resistance of oxide and mixture oxide optical coatings," Opt. Lett. **37**, 1478–1480 (2012).
25. J. B. Oliver, P. Kupinski, A. L. Rigatti, A. W. Schmid, J. C. Lambropoulos, S. Papernov, A. Kozlov, C. Smith, and R. D. Hand, "Stress compensation in hafnia/silica optical coatings by inclusion of alumina layers," Opt. Express **20**, 16596–16610 (2012) .
26. C. S. Menoni, E. M. Krous, D. Patel, P. Langston, J. Tollerud, D. N. Nguyen, L. A. Emmert, A. Markosyan, R. Route, M. Fejer, and W. Rudolph, "Advances in ion beam sputtered Sc_2O_3 for optical interference coatings," Proc. SPIE **7842**, 784202 (2010).
27. M. Mende, H. Ehlers, D. Ristau, and L. Gallais, "Laser damage resistance of ion-beam sputtered Sc_2O_3/SiO_2 mixture optical coatings," Appl. Opt. **52**, 1368–1376 (2013).
28. M. Mero, B. Clapp, J. C. Jasapara, W. Rudolph, D. Ristau, K. Starke, J. Kruger, S. Martin, and W. Kautek, "On the damage behavior of dielectric films when illuminated with multiple femtosecond laser pulses," Opt. Eng. **44**, 051107 (2005).
29. L. A. Emmert, M. Mero, and W. Rudolph, "Modeling the effect of native and laser-induced states on the dielectric breakdown of wide band gap optical materials by multiple subpicosecond laser pulses," J. Appl. Phys. **108**, 0435523 (2010).

1. Introduction

A main limitation in the development of high power ultrafast lasers is the peak power handling capability of the optical components. The available power of laser systems is indeed limited by laser damage to optical surfaces, particularly on the complex optical interference coatings that are used to control the reflection and transmission of the optics. This issue put enormous technological challenges on thin film devices and specific multilayer optical coatings that combine laser damage resistance with the ability to control pulse lengthening and spectral distortion. In a high power laser chain, the mirrors used for beam transport of the compressed beam to the application location are particularly submitted to the most severe irradiation conditions. These components should have a high reflection coefficient in a large spectral width, high laser damage threshold, low wavefront distortion, thermal and mechanical stability to enable high performances and stable operation under vacuum conditions. A physical way to overcome the physical limitation of laser damage is to enlarge the beam and increase the mirror surface. However, to reduce the technological challenges and cost to produce very large optics, there is a great interest to optimize optical designs.

Metal films, especially gold layers, play a significant role as mirrors in ultrafast laser systems because of the large available bandwidth but they have an intrisinc low laser induced damage threshold (LIDT) compared to multilayer dielectric mirrors [1]. However these last components are more difficult to design for large bandwidth reflection and low Group Delay Dispersion (3 or 4 materials can be needed) and to produce for large aperture systems (issues of inhomogeneities, mechanical stress,...). Different designs that combine mirrors with dielectric materials to take advantages of both systems have been proposed. In [2], Bonod et al. suggetsed to insert a metal layer between the substrate and the dielectric stack to reduce the number of dielectric bilayers and thus the mechanical stress within the stack. It was evidenced that this design with a metal layer is compatible with a high efficiency and high damage resistance under short pulse irradiation. So does Canova et al. [3] about the broad bandwidth of this design. In [4], Palmier et al. show that Metal MultiLayer Dielectric mirror (MMLD) have better performances than MultiLayer Dielectric Mirror (MLD) in optical properties such as larger bandwidth of reflectivity, while the damage threshold is almost the same as the MLD. Given the potential of such structures, and the fact that only very specific structures of MMLD have been studied up to now, we present in this paper a semi-analytical method that can be used to optimize the design of a MMLD to get the best balance between good optical performance and damage performance.

In the first part of this paper the model used to evaluate the temperature reached by a MMLD optical component under femto/pico second irradiation is detailed. We have investigated an approach, with different approximations that will be detailed, for the calculation of the transient temperature distributions in a multilayer system composed of dielectric and metallic films, submitted to single or multiple femtosecond pulses. It allows the determination of a theoretical thermal damage threshold of the system, defined as the fluence needed to reach the melting point of the metal. Then a discussion is conducted on the different materials and designs that can be used in the case of a MMLD mirror. And in the last part numerical results on the theoretical LIDT of different MMLD are given and discussed, to illustrate the interest of the approach.

2. Model of ultrashort pulse interaction with MMLD

The problem of the laser interaction with optical components has been largely studied for different geometries and irradiation conditions. The case of a bulk material for instance is a classical problem and a heat source in the material can be derived according to Beer-Lambert law to solve the heat equation [5]. For the case of optical interference coatings with absorbing layers, the problem of heat transfer and temperature rise in a stack has been studied for laser pulsed [6] and modulated [7] irradiation. However these approaches can not be applied to the specific case of a multilayer system like a Metal Multi-Layer Dielectric submitted to ultrafast laser irradiation. The geometry of the multilayer thermal problem under study in our work is shown in Fig. 1: the objective is to calculate the temperature distributions in space and time of optical interference coatings submitted to ultrashort and intense laser irradiations, with arbitrary temporal pulse shapes. A one-dimensional problem is considered since we are not interested in local laser heating but on the issues of laser damage of large optics. The limits to this simplification will be discussed in section 4. The case of single metal films, multi-layer metal films or protected metal films (metallic mirrors) is included in this approach.

2.1. Two Temperature Model (TTM)

In the case of ultrashort pulse irradiation, a detailed analysis of the energy deposition and transfer requires the modeling of the non-equilibrium processes. Indeed when the excitation time for laser heating is comparable to or shorter than the characteristic time of electron-phonon collision, the classical heat diffusion law is not applicable to describe the behaviors of the electron and lattice temperatures. To characterize this non-equilibrium process, a two temperature model

#186352 - $15.00 USD Received 4 Mar 2013; revised 24 Apr 2013; accepted 27 Apr 2013; published 13 Jun 2013

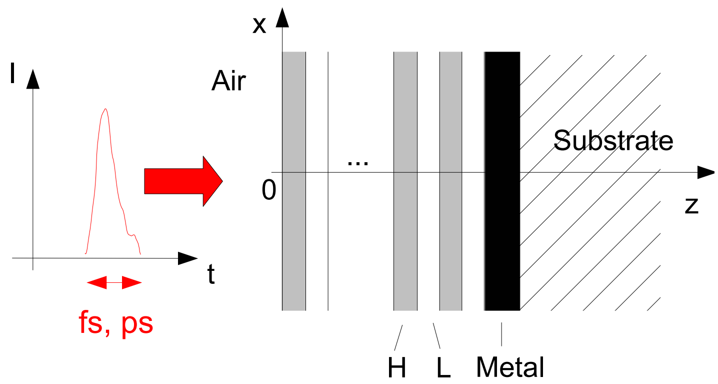

Fig. 1. Schematic and coordinates of the system under study. H: high refractive index layer, L: Low refractive index layer

can be used [8]. This model describes the energy transfer and the temperatures of electrons (T_e) and lattice (T_l) in a metal submitted to a laser irradiation at the femtosecond time scale. The incident laser energy directly excites the electrons localized within the skin depth. Then some part of the thermal electron energy transfers to the neighboring lattice, while another part of the energy diffuses, via electrons, into the deeper region of the material. When the ultrashort laser pulse is ended, the thermal coupling between the electrons and phonons as well as the heat conduction in the material will continue until equilibrium. These temperatures can be calculated by solving the coupled heat conduction equations of electrons and lattice:

$$C_e \frac{\partial T_e}{\partial t} = \nabla(K_e \nabla T_e)) - g(T_e - T_l) + S(z,t) \tag{1}$$

$$C_l \frac{\partial T_l}{\partial t} = \nabla(K_l \nabla T_l)) + g(T_e - T_l) \tag{2}$$

with C_e and C_l the specific heat capacities ($Jm^{-3}K^{-1}$) of the electrons and the lattice, respectively, K_e and K_l are the corresponding thermal conductivity coefficients ($Wm^{-1}K^{-1}$), the parameter g characterizes the rate of energy exchange ($Wm^{-3}K^{-1}$) between the electron and lattice subsystems, and S(z,t) is the heat source term induced by the laser irradiation (Wm^{-3}). The electronic heat capacity, thermal conductivity and electron-phonon coupling factor are dependent on the electronic temperature. These dependencies are complex and numerical electronic structure calculations are required to obtain their knowledge. Under moderate laser excitation (we are interested in the onset of damage and not in the strong ablation regime) simple analytical functions can be used: $C_e(T_e) = C_e' T_e$, $K_e = K_l \times T_e/T_l$ [10], but in the case of high electronic temperature, numerical expressions need to be used [11]. The source term can be written as $S(z,t) = K\alpha \left|E(z)\right|^2 nI_0 f(t)$, with α the absorption coefficient of the material, $\left|E(z)\right|^2$ the normalized electric field intensity (NEFI) in the material, which can be obtained from the Maxwell equations and the characteristic matrix of the film [9], n is the real part of the refractive index, I_0 is the laser energy density of the pulse (J/m^2) and f(t) a normalized function describing the laser temporal profile. In the following we will use a Gaussian pulse: $f(t) = \sqrt{4ln2/\pi} exp\left[-4ln2(t-2t_p)^2/t_p^2\right]$. The laser pulse is assumed to start at $t = 0$ and end at $t = 4t_p$. The laser energy outside this period of time is neglected since it is too small to signif-

#186352 - $15.00 USD Received 4 Mar 2013; revised 24 Apr 2013; accepted 27 Apr 2013; published 13 Jun 2013

icantly alter the results. Here, K is introduced to adjust the absorption. It takes into account the different physical mechanisms that can alter the laser energy deposition in the heated sample. For instance it was reported that there are transient changes of the film reflectivity during laser irradiation of metals [12, 13] and hence transient absorption variations during the irradiation. This value can be obtained by a comparison between calculations and experiments, and in the theoretical work that is described here it has been set to 1.

In order to solve the heat equations, we used a numerical partial differential equation solver [14]. A simulation of the case of a 500fs pulsed laser irradiating a single gold film on a silica substrate has been calculated as an example. The temperature profiles of electrons and lattice are shown in Fig. 2 at different timescales.

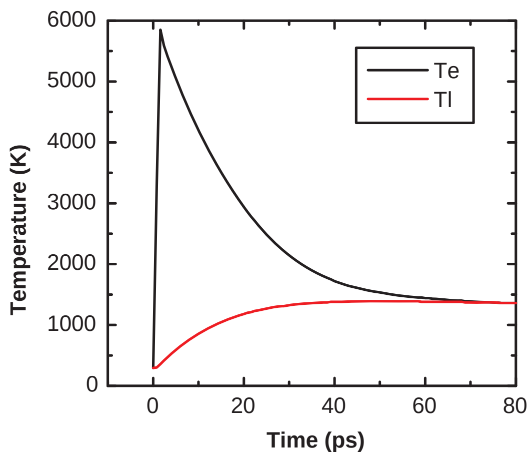

Fig. 2. Calculated temperature profiles (T_e: electronic temperature, T_l: lattice temperature) at the surface of a gold film irradiated by a pulsed laser. Laser wavelength is 800nm, pulse duration is 500fs and the fluence is $0.85J/cm^2$. The gold film thickness is 100nm, and the substrate is silica.

The electron temperature and lattice temperature reach equilibrium at a long time after the laser pulse. This corresponds to a critical time (t_c) that can be estimated by [10]:

$$t_c = \left(\frac{8}{\pi}\right)^{\frac{1}{4}} \left(\frac{C_l^3}{C_e' g^2 T_m}\right) \tag{3}$$

Depending on the material, t_c is in the range of 1-100 ps.

In Fig. 3 we have plotted the case of a multidielectric mirror with the following design: $silica/metal/(SiO_2/HfO_2)^4$, calculated with the procedure described above. The light is absorbed in the metal film embedded in the stack and then generated heat diffuses in the dielectric materials. Depending on the pulse repetition rate, the next pulse will be incident on a hot area and thermal accumulation effects can take place.

In the case of an optical component submitted to multiple pulses, damage can occur due to heat accumulation effects: the component does not have time to cool to the ambient temperature between each pulse. This effect is dependent on the repetition rate and the thermal conductivities of the different layers in the stack. If we want to deal with this problem of laser

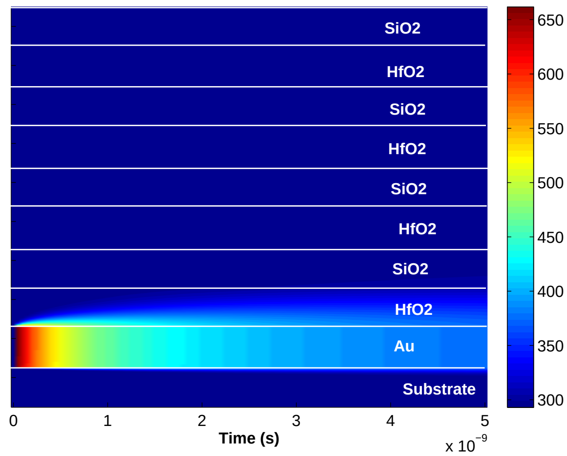

Fig. 3. Calculations of the lattice temperature with the two temperatures in the case of a metal multidielectric mirror composed of a dielectric mirror ($(HfO_2/SiO_2)^4$) on a gold film, deposited on a silica substrate. The laser irradiation is $4J/cm^2$ with a pulse duration of 500fs at 800nm. The temperature in the stack is plotted as a function of time up to 5ns after the end of the pulse in order to observe the temperature decay and diffusion.

accumulation and calculate the lattice temperatures, the source term in Eq. 1 can be written as:

$$S(z,t) = S_{1pulse}(z,t) * \sum_{n=1}^{n=N} \delta(t - nT) \tag{4}$$

with $S_{1pulse}(z,t)$ the heat source due to the absorption of a single pulse, $*$ the convolution operator, δ the Delta function, and F=1/T the laser repetition rate. The procedure to solve the heat equations is the same that in the previous case. The size of the calculation domain (air gap and substrate thickness) is dependent on the irradiation time. It is chosen large enough to prevent heating at the boundaries of system. Figure 4 shows the temperature evolution in a MMLD mirror submitted to high-repetition multiple pulses. This example shows an accumulation effect after a series of laser pulses at 1MHz that will induce thermal damage.

3. Materials and designs

In order to build a MMLD mirror, different metal and dielectric materials are available as well as different possibilities for the choice of the design. Then we review in this section the different materials available, their measured laser damage resistance, and the material parameters that can be used for simulation.

3.1. Choice of metal films

Metallic materials for ultrashort high power applications require high reflectance on a large bandwidth, and low absorption. The properties of the most common metals that can be used as reflecting coatings are shown in Fig. 5.

From these data we can see that aluminum has a good ultraviolet, visible and far infrared reflectance. However, the reflectance of aluminum drops significantly at wavelength 700 nm -900 nm which we are caring about. It makes aluminum out of consideration in this paper. Also for metal Nickel and Platinum, the reflectance is relatively too small to serve as a material that

#186352 - $15.00 USD Received 4 Mar 2013; revised 24 Apr 2013; accepted 27 Apr 2013; published 13 Jun 2013

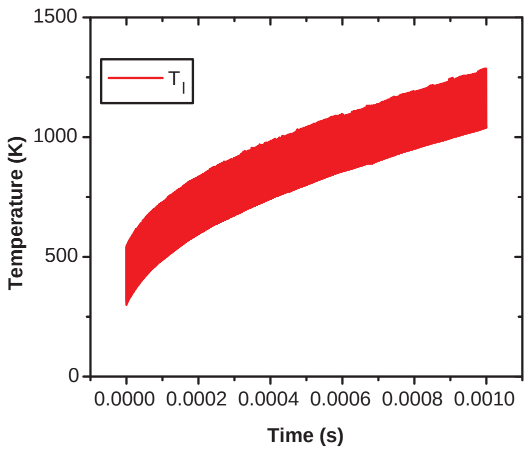

Fig. 4. Temperature evolution as a function of time of a metal/multidielectric stack (same design as in Fig. 3) submitted to multiple pulses irradiation. The temperature is plotted in the metal film, where it reaches its maximum value. The irradiation conditions are: pulse duration of 500fs, 1MHz repetition rate, $3.5J/cm^2$ per pulse, and 800nm wavelength.

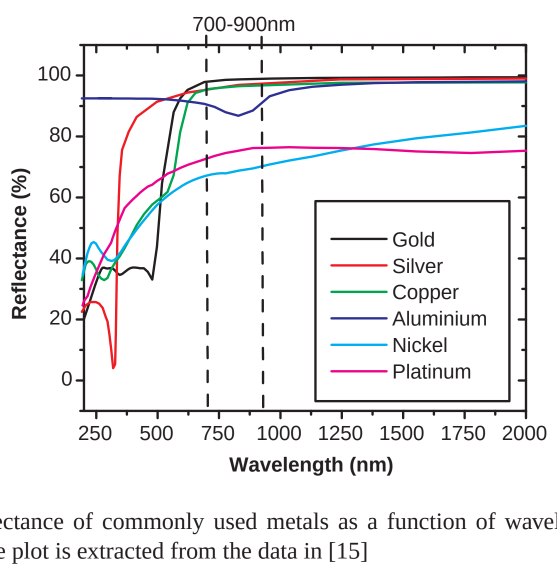

Fig. 5. Reflectance of commonly used metals as a function of wavelength from 200 to 2000nm. The plot is extracted from the data in [15]

#186352 - $15.00 USD Received 4 Mar 2013; revised 24 Apr 2013; accepted 27 Apr 2013; published 13 Jun 2013

can be a reflective mirror. Silver is one of the commonly used metal in optical applications [16] due to high reflectance and ease of evaporation. Though there are some oxidation issues when exposed to the atmosphere, this effect will be avoided when used in a MMLD because the dielectrics on the top of metallic film can protect it from the air. Thus, apart from laser damage resistance considerations, silver will be a very good choice for MMLD mirrors. Gold and copper are almost the same for infrared spectrum and they are good for infrared reflecting coatings beyond 700 nm. On glass, gold tends to form rather soft, easily damaged films, but a film of chromium or nichrome can solve this problem and make it adhere strongly to the substrate [16]. Energetic deposition processes can also improve the adhesion of gold on glass and make it applicable in the metal mirrors.

From the above discussions, gold, silver and copper are selected for further analysis. For these materials, we have collected some reported data about the damage thresholds (see Table 1) and parameters for calculations (Table 2).

Table 1. Summary of ultra-short laser damage thresholds of metal films and bulk materials, in the case of single shot irradiation and in normal incidence

Samples		**Test conditions**	**LIDT**	**Ref.**
Film / substrate	thickness (nm)	Wavelength, pulse duration	(J/cm^2)	
Gold / fused silica	100	400nm, 200fs	0.025	[17]
	300		0.058	
	500		0.095	
	700		0.11	
	900		0.112	
	1500		0.113	
Gold / BK7	31	793nm, 28fs	0.109	[18]
	51		0.189	
	70		0.23	
	90		0.33	
	135		0.39	
	147		1.11	
	295		2.11	
	900		2.84	
Silver / borosilicate	200	800nm, 120fs	≈0.9	[19]
Silver / BK7	not given	1054nm, 400fs	0.69	[20]
Silver / Kapton ®	100	1030nm, 500fs	1.1	[21]

A comparison of the theoretical damage thresholds of copper, gold and silver films with different thicknesses is reported on Fig. 6. The threshold is defined in simulations as the fluence needed to reach the melting point of the lattice, which is an arbitrary but convenient criterion for the comparison of materials. The calculations are done in the case of single pulse irradiation, and for a silica substrate.

Different comments can be made on these calculations. First of all the LIDT (melting) threshold saturates for each material, and when the film is thin the LIDT increases linearly with the

#186352 - $15.00 USD Received 4 Mar 2013; revised 24 Apr 2013; accepted 27 Apr 2013; published 13 Jun 2013

Table 2. Material parameters used in the TTM calculations.

Material	Gold	Silver	Copper
Refractive index [15]	0.08-4.6i	0.27-5.7i	0.25-5.2i
Lattice thermal conductivity [15]	$320WK^{-1}m^{-1}$	$430WK^{-1}m^{-1}$	$400WK^{-1}m^{-1}$
Lattice volumetric heat capacity [15]	$2.5\times10^{6}Jm^{-3}K^{-1}$	$2.5\times10^{6}Jm^{-3}K^{-1}$	$3.5\times10^{6}Jm^{-3}K^{-1}$
Diffusivity	$1.28\times10^{-4}m^{2}s^{-1}$	$1.72\times10^{-4}m^{2}s^{-1}$	$1.14\times10^{-4}m^{2}s^{-1}$
Melting point [15]	$1064^{o}C$	$962^{o}C$	$1085^{o}C$
Electron heat capacity [11] ($Jm^{-3}K^{-1}$)	$67.6\times T_e$ for $T_e\leq2000K$	$63.3\times T_e$ for $T_e\leq4000K$ values from [11] above	$96.8\times T_e$ for $T_e\leq2000K$
Electron phonon coupling coefficient [11] ($Wm^{-3}K^{-1}$)	2.5×10^{16} for $T_e\leq3000K$	1.5×10^{16} for $T_e\leq5000K$ values from [11] above	5×10^{16} for $T_e\leq3000K$
Electron thermal conductivity ($Wm^{-1}K^{-1}$)	$K_e=\frac{v_F^2}{3}\frac{C_e(T_e)}{BT_l+AT_e^2}$ $A=1.2\times10^{7}K^{-2}s^{-1}$, $B=1.23\times10^{11}K^{-1}s^{-1}$ [22]	$K_e=K_l\frac{T_e}{T_l}$	$K_e=K_l\frac{T_e}{T_l}$

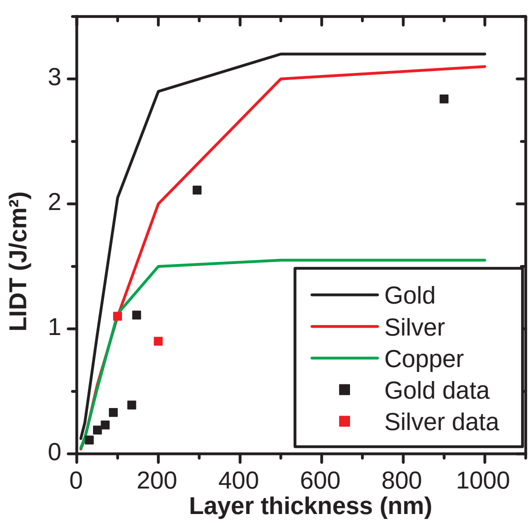

Fig. 6. Theoretical thresholds for single layer metal film with different thicknesses, calculated at 800nm, 50fs, using the material parameters listed in table 2. The experimental data correspond to the values given in table 1.

#186352 - $15.00 USD Received 4 Mar 2013; revised 24 Apr 2013; accepted 27 Apr 2013; published 13 Jun 2013

film thickness. This has been observed experimentally for the case of gold (see values of Table 1) and the limit between the two domains can be defined as L_c. This length is characteristic of the heat penetration depth and related to the thermal parameters of the materials and the strength of the electron-phonon coupling. Numerical simulations indicate that L_c is around 200nm for copper, 400nm for silver and 300nm for gold in the case of single pulse irradiation. An optimized design should then consider a metal thickness higher than L_c. The second point of interest is the comparison of the LIDT values between the different materials. Obviously gold and silver should be preferred to copper. Given the lack of available experimental data on these two materials, it is difficult to conclude on which material (gold or silver) would have the better laser damage resistance. The available experimental data are reported on Fig. 6. The pulse duration for calculations and experiments are not the same, but this parameter has minor influence on the results. It can be observed for gold a discripency between experiments and theory. This can be the result of a difference between real parameters of the film (that can be different from the bulk) and theoretical parameters, or a theoretical damage threshold definition that is not well adapted (damage can occur before melting, with spallation mechanisms). However, since our present study is theoretical and that there are not sufficient published experimental data to conclude, we will use the values given in Table 2 in the following.

3.2. Choice of dielectric films

In the case of dielectric materials, because the damage is the consequence of photoionization and impact ionization, physical mechanisms for which the efficiency depends on the bandgap of the material, the LIDT is directly dependent on the bandgap value. In the case of bulk materials, fluorides have a better laser damage resistance than oxides [1]. In the case of thin films however this is not the case and only the oxides have shown a clear scaling of laser damage threshold with the bandgap: a linear scaling of the breakdown fluence with band gap energy is observed for a large range of materials [23]. In the case of mixture of oxides however, more complex dependencies were observed [24]. In this work we will then use only simple oxides as the low and high index materials. For the low index material silica is the obvious choice. The damage threshold of this material has been measured between 4 and $4.5J/cm^2$ at 500fs [23, 24] at 800nm or 1030nm (notice that results at these two wavelengths are comparable since the photon energies are very close). We will take the value of $4J/cm^2$ for silica as a conservative choice and use the empirical laws described by Mero et al. [23] for the pulse duration dependence.

For the high index material there are different alternatives. Hafnium oxide (HfO_2) is one of the most important high index materials for the production of optical multilayer coatings for UV to IR high power applications. In addition to its good optical and mechanical properties, it has a relatively high laser-induced damage threshold (LIDT) compared to other materials (Ta_2O_5, Nb_2O_5, ZrO_2). According to [23, 24] the laser damage threshold is $1.6J/cm^2$ at 500fs. Aluminum oxide (Al_2O_3) with a higher bandgap than the one of hafnium oxide is another interesting choice. Although the refractive index for Al_2O_3 is lower than the one for HfO_2, the LIDT is significantly higher ($2.5J/cm^2$ at 500fs [23, 24]). With the drawback of larger number of layer pairs, the use of Al_2O_3/SiO_2 can be a good alternative to HfO_2/SiO_2. More efficient designs should use the three materials (Al_2O_3, HfO_2, SiO_2), which can also be beneficial to obtain low stressed multilayer systems [25]. Scandium oxide is also an attractive candidate with a high refractive index and a relatively large bandgap although it has not been widely explored [26]. Recent results suggest that a higher laser damage resistance could be obtained compared to HfO_2 and SiO_2 [27], but it will not be used in our theoretical study given the lack of other data. Following this analysis, SiO_2, HfO_2 and Al_2O_3 will be used as the low and high index materials.

#186352 - $15.00 USD Received 4 Mar 2013; revised 24 Apr 2013; accepted 27 Apr 2013; published 13 Jun 2013

4. Numerical results: comparison between MMLD and dielectric mirrors

In this section the theoretical LIDT of dielectric mirrors is compared to MMLD mirrors composed of a metal film and a dielectric mirror. The thickness of the metal film will be chosen based on the calculation presented in the previous section, in order to optimize the LIDT. The objectives are to determine the number of dielectric bilayers that need to be deposited on the metal film in order to achieve a higher LIDT than dielectric mirrors, better GDD and higher bandwidth. An example of the comparison of the optical properties of such mirrors is given in Fig. 7.

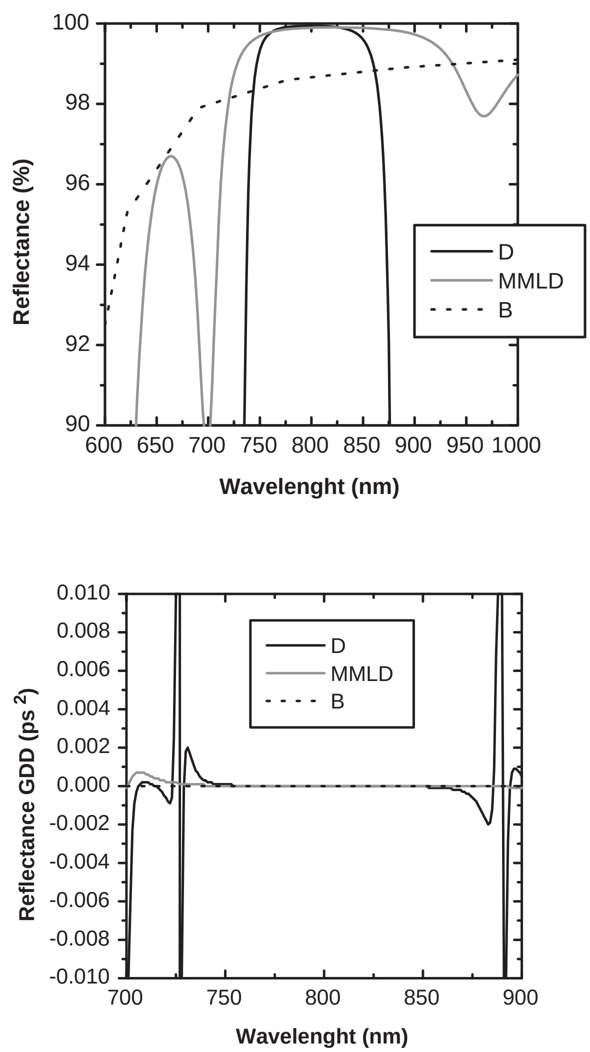

Fig. 7. A comparison of the Reflectance and Group Delay Dispersion of a dielectric mirror $Silica/(HfO_2/SiO_2)^{15}/HfO_2$ (D), a MMLD mirror $Silica/Gold/(SiO_2/HfO_2)^5$ (M), and a metallic gold mirror (B).

#186352 - $15.00 USD Received 4 Mar 2013; revised 24 Apr 2013; accepted 27 Apr 2013; published 13 Jun 2013

4.1. Case of single pulse irradiation

In the case of a dielectric stack, the LIDT is limited by one of the materials that compose the stack and it can be evaluated based on the electric field distribution in the stack under consideration. One can calculate the theoretical damage threshold with :

$$LIDT_{stack} = |E_{inc}/E_{max}|^2 \times LIDT_{material} \tag{5}$$

The theoretical damage threshold of the dielectric part of the MMLD can be calculated in the same way. Based on this simple calculation it is possible to compare the fluence that will damage the dielectric films with the fluence that will melt the metal and calculated with the method detailed in this paper. As an illustration, the E-field distribution in a mirror with the design $Silica/Gold/(SiO_2/HfO_2)^5$ is given in Fig. 8.

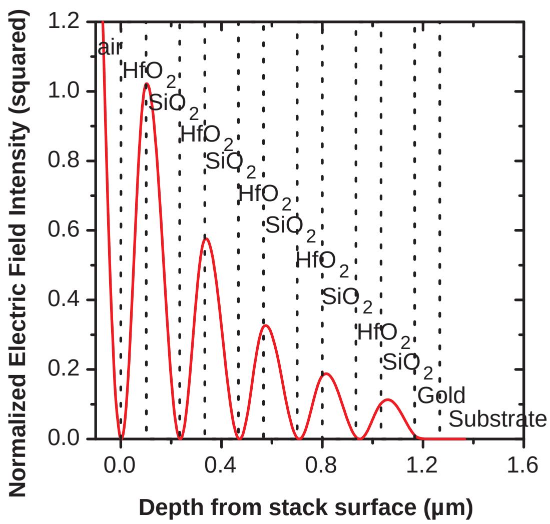

Fig. 8. Electric field distribution in the stack $Silica/Gold/(SiO_2/HfO_2)^5$, calculated at 800nm.

In the case of the design given in Fig. 8, the limiting film is the upper high index layer of HfO_2 and considering the intrinsic LIDT of hafnia ($1.6J/cm^2$ at 500fs) we found that the film will break at an incident fluence on the mirror of $1.4J/cm^2$. At such fluence we found from calculation that the metal film will be far from melting ($12.8J/cm^2$ for instance is needed to reach the melting point of a 100nm gold layer in this design) and the limiting film is the dielectric high index material. In this configuration the metal film can be less than L_c.
Using such a methodology it has been possible to calculate the theoretical LIDT of different MMLD mirrors as a function of the number of dielectric layers and thickness of the metal films, and identify the limitation (metallic or dielectric film). Calculations are shown in Fig. 9 for two different MMLD mirrors.

From these calculations we can conclude that in the case of a MMLD mirror composed of few bilayers (2 or 3) the fluence needed to reach the melting point of the metal is higher than the fluence needed to damage the high index material. A design with 5 bilayers has then good optical properties for a high reflective mirror with low GDD compared to an all dielectric design (see Fig. 7) and the LIDT is not limited by the metal. However these conclusions are based only

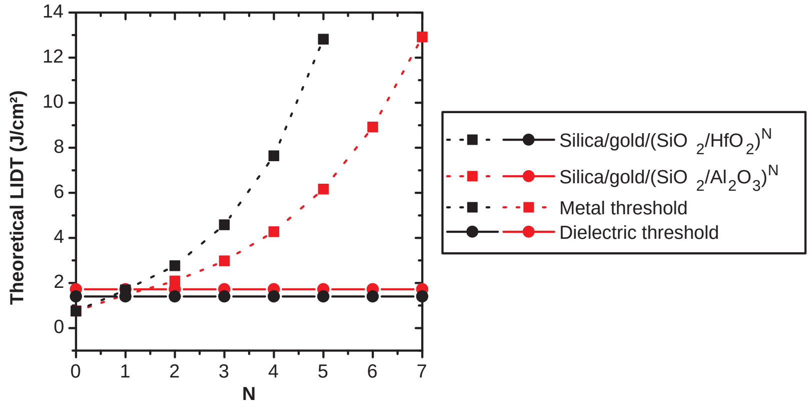

Fig. 9. Case of MMLD mirrors with different high index materials: calculation of the fluence needed to reach the melting point of the gold film (dotted lines) and comparison to the fluence needed to initiate damage in the high index material (plain line).

on the analysis of single pulse irradiation and are valid for low repetition rate irradiation. The heat accumulation for the case of multiple pulses can decrease the threshold depending on the pulse repetition rate. We will evaluate these effects in the next section.

4.2. Case of multiple pulses

To illustrate the effects of multiple pulse laser heating we have plotted on Fig. 10 the calculated fluence needed to reach the melting point of the metal layer in a MMLD mirror (5 dielectric bilayers in this case) for different repetition rates and number of pulses.

When the pulse repetition rate increases there is less time between two successive shots for the heated region to cool to the ambient temperature. As it was shown in Fig. 4, the heat is accumulated in the stack up to the point when thermal breakdown of the structure can occur. The calculations reported on Fig. 10 shows that for moderate repetition rates (less than 1kHz) the theoretical melting threshold of the metal film is one order of magnitude higher than the fluence needed to reach the breakdown of the dielectric films in the stack. In such conditions of operations the MMLD mirrors can operate safely. However this MMLD design is not adapted to the case of multiple pulses irradiations with high repetition rates: at 1MHz the melting threshold of the film reaches the damage threshold of the diectric films in the order of 10000 to 100000 pulses (0.01 to 0.1 seconds).

The approach described in this paper can then provide useful information on intensity and frequency range where the mirrors can operate safely. However they are different limitations that should be clearly recalled. A simplification to a one dimensional problem (z coordinate) has been considered which implies that the thermal conduction out of the irradiated must be negligible, i.e. the beam radius must be much larger than the heat diffusion length in the transverse dimension of the metal film (x,y). From first order thermal calculations this condition is fulfilled for:

$$t_i << R^2/D \tag{6}$$

with t_i the irradiation time, R the beam radius and D the diffusivity. Considering the diffusivity of a metal film ($10^{-4}m^2s^{-1}$), the limitation is 10ms for R=1mm, 1s for R=1cm and 100s for

#186352 - $15.00 USD Received 4 Mar 2013; revised 24 Apr 2013; accepted 27 Apr 2013; published 13 Jun 2013

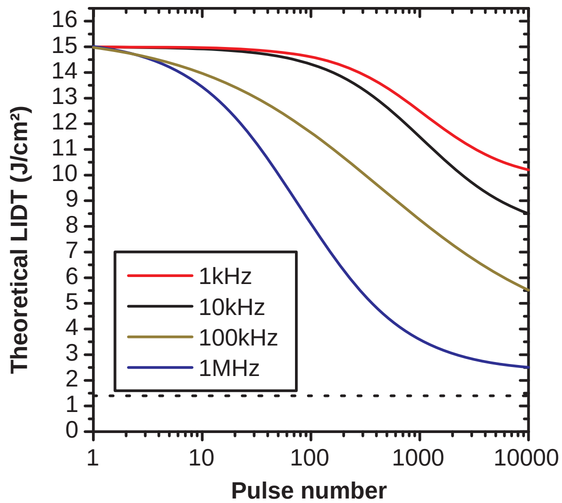

Fig. 10. Calculation of the fluence needed to reach the melting point of the gold film in the case of a MMLD mirror ($Silica/Gold/(SiO_2/HfO_2)^5$) irradiated with different number of laser pulses at various repetition rates. The dotted line corresponds to the fluence needed to initiate damage in the high index material of the stack.

R=10cm. Secondly, non-linear ionization processes in the dielectric films could contribute to the temperature increase of the stack and should be taken into account in future works. Another limitation is the fact that the decrease of the dielectric LIDT when illuminated with multiple pulses should be taken into account. For a more complete description, a refined model should integrate: non-linear absorption mechanisms (photo and impact ionization) leading to temperature increase [28], the accumulation of photo-induced defects leading to a decrease in threshold [29] or ripples formation at the stack surface [4]. These mechanisms should lead to a decrease in the LIDT of the dielectric films depending on the repetition rate and pulse number. Therefore the dotted line within the Fig. 10 should be considered as an upper limit for the dielectric LIDT.

5. Conclusion

Under short pulse and high repetition rate laser irradiation multilayer stacks composed of dielectric and metallic films can be damaged due to thermal effects. The thermal consequences due to the ultrafast absorption of energy in the metal film and heat diffusion in the stack can be evaluated with the approach that has been described. In this case theoretical damage threshold in the condition of operation can be obtained and the design, as the choice of the materials can be optimized.

Several examples were analyzed in this paper and it was shown for instance that in the case of single shot and low to moderate repetition rate (less than 1kHz)) the damage threshold of a MMLD mirror involving gold or silver films is not limited by the metal but by the dielectric materials. In the case of high repetition rates (100kHz, 1MHz) however thermal damage of the optical component can take place, depending on the duration of the burst of pulses.

The theoretical work that has been presented is now intended to be applied to practical studies in order to compare the results with experiments.